

Probing features in inflaton potential and reionization history with future CMB space observations

Dhiraj Kumar Hazra,¹ Daniela Paoletti,^{2,3} Mario Ballardini,^{4,2,5,3} Fabio Finelli,^{2,3} Arman Shafieloo,^{6,7} George F. Smoot,^{1,8,9,10} Alexei A. Starobinsky^{11,12}

¹AstroParticule et Cosmologie (APC)/Paris Centre for Cosmological Physics, Université Paris Diderot, CNRS, CEA, Observatoire de Paris, Sorbonne Paris Cité University, 10, rue Alice Domon et Leonie Duquet, 75205 Paris Cedex 13, France

²INAF/IASF Bologna, via Gobetti 101, I-40129 Bologna, Italy

³INFN, Sezione di Bologna, via Irnerio 46, I-40127 Bologna, Italy

⁴Department of Physics & Astronomy, University of the Western Cape, Cape Town 7535, South Africa

⁵Dipartimento di Fisica e Astronomia, Università di Bologna, Viale Berti Pichat, 6/2, I-40127 Bologna, Italy

⁶Korea Astronomy and Space Science Institute, Daejeon 34055, Korea

⁷University of Science and Technology, Daejeon 34113, Korea

⁸Institute for Advanced Study & Physics Department, Hong Kong University of Science and Technology, Clear Water Bay, Kowloon, Hong Kong

⁹Physics Department and Lawrence Berkeley National Laboratory, University of California, Berkeley, CA 94720, USA

¹⁰Energetic Cosmos Laboratory, Nazarbayev University, Astana, Kazakhstan

¹¹Landau Institute for Theoretical Physics RAS, Moscow, 119334, Russian Federation

¹²Kazan Federal University, Kazan 420008, Republic of Tatarstan, Russian Federation

E-mail: dhiraj.kumar.hazra@apc.univ-paris7.fr, paoletti@iasfbo.inaf.it,
mario.ballardini@gmail.com, finelli@iasfbo.inaf.it, shafieloo@kasi.re.kr,
gfsmoot@lbl.gov, alstar@landau.ac.ru

Abstract. We consider the prospects of probing features in the primordial power spectrum with future Cosmic Microwave Background (CMB) polarization measurements. In the scope of the inflationary scenario, such features in the spectrum can be produced by local non-smooth pieces in an inflaton potential (smooth and quasi-flat in general) which in turn may originate from fast phase transitions during inflation in other quantum fields interacting with the inflaton. They can fit some outliers in the CMB temperature power spectrum which are unaddressed within the standard inflationary Λ CDM model. We consider Wiggly Whipped Inflation (WWI) as a theoretical framework leading to improvements in the fit to the Planck 2015 temperature and polarization data in comparison with the standard inflationary models, although not at a statistically significant level. We show that some type of features in the potential within the WWI models, leading to oscillations in the primordial power spectrum that extend to intermediate and small scales can be constrained with high confidence (at 3σ or higher confidence level) by an instrument as the Cosmic ORigins Explorer (CORE). In order to investigate the possible confusion between inflationary features and footprints from the reionization era, we consider an extended reionization history with monotonic increase of free electrons with decrease in redshift. We discuss the present constraints on this model of extended reionization and future predictions with CORE. We also project, to what extent, this extended reionization can create confusion in identifying inflationary features in the data.

Contents

| | | |
|----------|--|-----------|
| 1 | Introduction | 1 |
| 2 | Inflation and the primordial power spectrum | 3 |
| 2.1 | Wiggly Whipped Inflation | 3 |
| 2.1.1 | Discontinuity in the potential | 3 |
| 2.1.2 | Discontinuity in the derivative of the potential | 4 |
| 3 | Forecasts for WWI | 4 |
| 3.1 | WWI and WWI' numerical set up | 5 |
| 3.2 | Priors for WWI and WWI' | 5 |
| 3.3 | CORE specifications | 6 |
| 3.4 | Forecasts for primordial features | 7 |
| 4 | Reionization history | 11 |
| 4.1 | Solving for reionization | 12 |
| 4.2 | Constraints on Reionization history | 12 |
| 5 | Confusion between inflationary features and extended reionization history | 15 |
| 6 | Conclusions | 18 |

1 Introduction

With its nine frequency channels, Planck has probed the CMB anisotropy pattern with unprecedented accuracy and has provided the tightest constraints on cosmological parameters [1, 2] and on the primordial power spectrum (PPS) from the simplest models of inflation [3]. The Planck 2015 data are statistically consistent with a power law form for the PPS [3] and with Gaussian perturbations [4], which are both compatible with the predictions of standard single field slow roll inflation models.

Although not at a statistically significant level, an improved fit to the temperature power spectrum by Planck [3, 5–7] can be obtained by features in the PPS as provided by temporary violation of the slow-roll condition during inflation produced by non-smooth pieces in an inflaton potential (smooth and quasi-flat in general). The Wiggly Whipped Inflation (WWI) has provided a framework for classes of model with primordial features which improves the fit to the Planck 2015 data with respect to the power law model [8, 9]. These features can be localized on certain scales or they can represent wiggles over a wide range of cosmological scales. Within the WWI framework, we consider inflationary phase transitions where the scalar field rolls from a steeper potential into a nearly flat potential through a discontinuity in the potential or in its derivative. We obtained five types of features that provide a $\Delta\chi^2 \sim 12 - 14$ improvement, compared to the power law, in the fit to the Planck data, with the addition of 2-4 extra parameters depending on the model. These features help improve the fit to the Planck 2015 temperature and polarization anisotropies separately and in combination. Four types of features come from the model where we have a (smoothed) discontinuity in the potential. The remaining type is instead generated by

a discontinuity in the first derivative of the potential. The baseline potential used in the latter case is the α -attractor model [10], in a limit where it reduces to Starobinsky $R + R^2$ model [11]. Since a large fraction of inflation models belong to a universal class where spectral tilt and tensor amplitude follow the same function of e -folds, it is interesting to use such potential in a framework for generating features. Since the release of WMAP data, different features have been tested with the data, such as features generated with a step in the inflaton potential or in its first derivative [12–14], oscillations in the inflaton potential [15] or through an inflection point [16] *. Several reconstruction of the PPS from the CMB have demonstrated [18] the hints of suppression of power and oscillations at large and intermediate scales ($\ell \lesssim 40$) and sharper oscillations that continues to small scales. As mentioned before, given the uncertainties in the CMB data associated at different scales, while these features are not statistically significant, they are interesting because of following three reasons: firstly, some of these features are consistently present since WMAP observations [19–22]; secondly, Planck temperature and polarization observations jointly support these features; and finally, within a single framework of inflation, WWI, these three classes of features can be generated at the required cosmological scales [9].

The main goal of this paper is to investigate what a future concept for space mission dedicated to CMB polarization can tell about the existence of features as generated by a temporary violation of the slow-roll condition during inflation. We focus on space missions because only space experiments can observe the full sky and therefore access the largest angular scales. We consider for our forecast the CORE proposal [23–27] as a concept for a future CMB polarization dedicated space mission [28–30]. The study presented here is complementary to the CORE forecasts for primordial features presented in [27].

Along with forecasting the capabilities of a future mission as CORE regarding primordial features, we will also investigate the current constraints on the reionization history and the corresponding CORE forecasts. Beyond the interest in the process of reionization per se, there is an additional reason to investigate this specific topic in this paper. Indeed, large scale features in the PPS are degenerate to some extent with extended reionization histories in the CMB polarization spectrum: it is therefore important to investigate the effect of this degeneracy in the constraints on primordial features, in particular in the perspective of future high accuracy polarization data. There are still grey areas in the knowledge of the process of reionization: in particular, the details of the transition from neutral hydrogen to a fully reionized medium (for $z > 6$) are still unknown, and nevertheless they affect the large angular scale CMB polarization pattern and have consequences on the determination of cosmological parameters.

Attention has been already paid in the past [31] to the degeneracy between primordial features and reionization. Using the Principal Components as basis for parametrizing general reionization histories, it has been demonstrated that complex reionization histories [32] can reduce the significance of primordial features for a non-standard inflationary model with a step in a quadratic potential [31]. Keeping this in mind, in this paper we use a one parameter controlled reionization history that allows more freedom than a Tanh step (that is usually assumed in the Einstein-Boltzmann codes), but at the same time does not allow a complete free form reionization history as in PCA. Also this parametrization does not allow unphysical reionization histories. We consider a monotonic increase in neutral hydrogen fraction with

* Another possibility to obtain localized oscillatory features in the primordial scalar power spectrum which we do not consider in this paper is a transient change in the inflaton effective sound speed [17] that may occur during multiple inflation.

redshift and we provide the constraints with Planck 2015 data and the forecast for CORE capabilities. We also discuss the degeneracy between the reionization history and a particular shape of large scale power spectra supported by Planck data.

The paper is organized as follows: in section 2 we review the WWI potential. We first summarize the features that are supported by Planck 2015 data [9], we introduce a minor change in the WWI parametrization with respect to previous treatments. In section 3 we provide all the necessary details for the analysis and present the results. In the reionization dedicated part 4, we discuss the different parametrizations, both the commonly used model and the one utilized in this paper. We present the methodology and priors, together with the constraints we obtained. In section 5 we provide our study of the degeneracies between the primordial power spectrum and extended reionization histories. We conclude in section 6.

2 Inflation and the primordial power spectrum

We start with the discussion of the WWI framework, in a slightly modified form with respect to previous treatments, and the Planck 2015 results.

2.1 Wiggly Whipped Inflation

In the WWI framework the potential is described by:

$$V(\phi) = V_S(\phi) + V_R(\phi), \quad (2.1)$$

where, V_R is the steep part which merges into the slow roll part V_S with or without a discontinuity. This steep to flat phase transition in inflation allows features in the PPS on cosmological scales. In the literature [12, 33–38] the possibility of a phase transition in the inflaton potential has been discussed within different frameworks. The WWI one, in particular, allows the potential and/or its derivatives to have discontinuities.

2.1.1 Discontinuity in the potential

We use the WWI potential as provided below in Eq. 2.2:

$$V(\phi) = V_0 \left[\left(1 - \left(\frac{\phi}{\mu} \right)^p \right) + \Theta(\phi_T - \phi) (\gamma(\phi_T - \phi)^q + \phi_0^q) \right], \quad (2.2)$$

where we note that $V_S(\phi) = V_0 \left(1 - \left(\frac{\phi}{\mu} \right)^p \right)$ has 2 parameters, V_0 and μ . μ and the index p determine the spectral tilt n_s and the tensor-to-scalar ratio r . We choose the values $p = 4$ and $\mu = 15 \text{ M}_{\text{PL}}$ such that $n_s \sim 0.96$ and $r \sim \mathcal{O}(10^{-2})$ (as in [14, 39]). With respect to the previous treatment, here we change a bit the steep part in the potential $V_R(\phi)$. It is composed by two independent part: $\gamma(\phi_T - \phi)^q$ which generates the whipped suppression [40] through the fast roll, and ϕ_0^q which introduces the wiggles through the discontinuity. Hence, the potential discussed in [9] is nested within this potential. The extent of the potential discontinuity is $\Delta V = V_0(\phi_0)^q$. We use $q = 2$ as in [9]. The transition and discontinuity happen at the same field value ϕ_T just like the old potential. In this case to have a featureless PPS it is necessary to have satisfied both $\gamma = 0$ and $\phi_0 = 0$. Separately, $\phi_0 = 0$ reduces the potential to Whipped Inflation form and $\gamma = 0$ reduces the potential to a form where we do not have large scale suppression in the PPS but we generate localized and non-local wiggles.

The Heaviside Theta function $\Theta(\phi_{\text{T}} - \phi)$ is modeled numerically as usual by a Tanh step ($\frac{1}{2} [1 + \tanh[(\phi_{\text{T}} - \phi)/\delta]]$) and thereby introduces a new extra parameter δ . Note that ϕ , ϕ_{T} and ϕ_0 are all measured in units of the reduced Planck mass.

With ‘WWI potential’, we shall refer to the potential in Eq. 2.2. The main advantage of using WWI potential is that within a single potential we can generate a multitude of features that are supported by the CMB data. It acts as a generic model to avoid the use of different potentials for parameter estimation.

2.1.2 Discontinuity in the derivative of the potential

With ‘WWI’ potential’ we shall refer to the potential with a discontinuity in the derivative which reads as follows:

$$V(\phi) = \Theta(\phi_{\text{T}} - \phi)V_0(1 - \exp[-\alpha\kappa\phi]) + \Theta(\phi - \phi_{\text{T}})V_1(1 - \exp[-\alpha\kappa(\phi - \phi_0)]). \quad (2.3)$$

This potential is same that has been used in [9], it is composed of α -attractor potentials [10] with different slopes appearing in the exponent, allowing a discontinuity in the derivative. Since in this case the potential is continuous,

$$V_0(1 - \exp[-\alpha\kappa\phi_{\text{T}}]) = V_1(1 - \exp[-\alpha\kappa(\phi_{\text{T}} - \phi_0)]), \quad (2.4)$$

and note that $V_1 > V_0$. $\kappa^2 = 8\pi G$ and we use the convention where it is equal to 1. The parameter α , that controls the slope of the potential, is fixed to $\sqrt{2/3}$ to reproduce the Starobinsky’s $R + R^2$ inflationary model [11] in the Einstein frame which gives a primordial tensor power spectrum with $r \sim 4 \times 10^{-3}$ for the featureless case. Within this treatment we have only two extra parameters compared to featureless case, ϕ_{T} (field value at the transition) and ϕ_0 (extent of the discontinuity in the derivative of the potential). Here too ϕ , ϕ_{T} and ϕ_0 are measured in units of the reduced Planck mass. The primordial feature from WWI’, as has been discussed in the previous paper on WWI, is similar to the original Starobinsky-1992 model [12].

In both the potentials given in Eq. 2.2 and 2.3, the tensor-to-scalar ratios are chosen to be in perfect agreement with the current upper bounds from the data but also in the ballpark of a possible detection by a CORE like survey. In [9] we identified four local minima of the Planck 2015 data, corresponding to likelihood peaks, where we observed an improvement in the fit compared with the power law in temperature/polarization data separately and in combination. We can identify these different types of local and global features as four broad categories: WWI-A, B, C and D. WWI’ having only 2 extra parameters provided a substantial improvement in fit to the Planck 2015 data. These four+one types of features are plotted in figure 1. With a CORE like survey, we mainly aim to address what is the expected significance of the features, and possibly to distinguish among the four WWI types, should one of them represent the true model of the Universe. In the case of WWI’ we have only one type of feature, therefore we address in this case to what extent we can reject the power law PPS with future CMB surveys, should the best fit WWI’ from Planck represent the true model of the Universe.

3 Forecasts for WWI

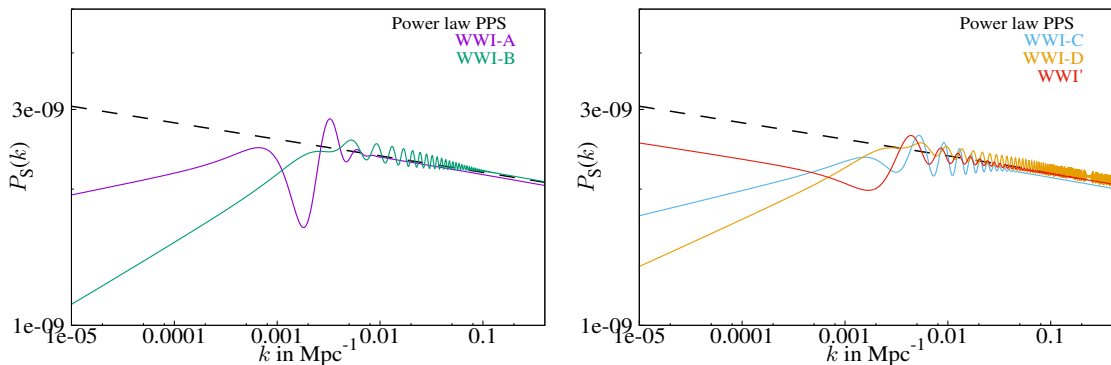


Figure 1. The best fit primordial power spectra obtained from Planck 2015 analysis with Wiggly Whipped Inflation model. Left plot shows WWI-A and B best fits and the right one shows WWI-C, D and WWI' best fits. Note the best fits WWI-[A, B, C, D] belong to the same potential. Best fit power law PPS is also provided in dashed black. The color codes for different best fits will be used consistently throughout the paper.

3.1 WWI and WWI' numerical set up

The numerical details regarding the solution to WWI models have been already discussed in earlier papers [8, 9, 40]. Hence, here we will only briefly mention the main codes that are used in this analysis. Publicly available code BI-spectra and Non-Gaussianity Operator, BINGO [41, 42] is used to generate the power spectra from WWI and WWI' inflationary models. The discontinuity in the potential is modeled with a Tanh step function with a width δ as explained before. We use the same initial values as has been used in Ref [9]. BINGO solves the background and Mukhanov-Sasaki equations using standard Bunch-Davies initial conditions and the initial value of scale factor is estimated by imposing that the $k = 0.05 \text{ Mpc}^{-1}$ mode leaves the Hubble radius 50 *e-folds* prior to the end of inflation.

We use publicly available CAMB and COSMOMC for our analysis. The codes are modified in order to incorporate the WWI through BINGO and the new reionization history. In standard Tanh reionization scenario, we use the baryon density ($\Omega_b h^2$), cold dark matter density ($\Omega_{\text{CDM}} h^2$), the ratio of the sound horizon to the angular diameter distance at decoupling (θ) and the optical depth (τ) as free parameters. Note that the standard *nearly instantaneous* reionization history is described by one parameter τ . These four parameters will be common to all the analyses in this paper. When using real data from Planck 2015 release we will allow also the foreground and nuisance parameters to vary according to the Planck likelihood set up. Extra parameters corresponding to inflationary models and reionization used in this paper will be mentioned in the subsequent sections.

3.2 Priors for WWI and WWI'

V_0 mainly dictates the amplitude of scalar perturbations and we have chosen a prior wide enough to ensure the convergence of the likelihood bounded from both ends. The field value corresponding to when the phase transition in inflation occurs, ϕ_T , is varied such that the features occur on the cosmological scales probed by an experiment like CORE. The potential parameter γ has priors that include no suppression (for $\gamma = 0$) and a value where the transition allows enough *e-folds* (~ 70) of inflation. Similarly, for ϕ_0 , that represents the amplitude of the wiggles in the PPS, we set the lower limit to zero, which corresponds to no wiggles. The higher limit is $\phi_0 = 0.04 M_{\text{Pl}}$ that shows oscillations (for all widths of transition

considered) that are large enough to be strongly disfavored by Planck 2015 data. $\ln(\delta)$ is varied from -12 to -3 that allow sufficiently sharp and wide transitions. For the WWI we calculate the angular power spectrum at all multipoles instead of interpolating, like usually done in numerical codes, in order to capture the sharp features.

3.3 CORE specifications

We now describe the methodology we use to forecast the capabilities of a concept for a future CMB space mission as CORE to constrain the primordial origin of the features. As fiducial cosmologies, we choose the WWI best-fits of the Planck 2015 temperature and polarization data [9]. We perform the CORE forecasts as described in [26, 27]. We use an inverse Wishart likelihood with an effective noise sensitivity and angular resolution obtained from an inverse noise weighted combination of the central frequency CORE channels whose specifications are:

$$\begin{aligned}
\text{Frequency [GHz]} &= \{130, 145, 160, 175, 195, 220\} \\
\text{FWHM [Arcmin]} &= \{8.51, 7.68, 7.01, 6.45, 5.84, 5.23\} \\
\Delta T [\mu\text{K arcmin}] &= \{3.9, 3.6, 3.7, 3.6, 3.5, 3.8\} \\
\Delta P [\mu\text{K arcmin}] &= \{5.5, 5.1, 5.2, 5.1, 4.9, 5.4\}
\end{aligned}
\tag{3.1}$$

We assume that systematic effects are subdominant and that foreground contaminations are kept under control by the lower 6 (down to 60 GHz) and higher 7 (up to 600 GHz) frequency channels [24, 25]. In addition to temperature and polarization anisotropies, we consider the CMB lensing potential power spectrum C_ℓ^{PP} , which an experiment like CORE will be able to reconstruct up to the scales where linear theory is reliable. As simulated noise spectrum in the lensing potential we use the EB estimator [43] as in [26, 27, 44].

Since we are investigating the possible constraints on features beyond the standard model in the primordial power spectrum with CORE, for comparison we present the 95% CL uncertainties expected from an experiment like CORE compared to the Planck 2015 results in the standard Λ CDM power law PPS:

$$\begin{aligned}
\text{Parameter} &= \{\Omega_b h^2, \Omega_{\text{CDM}} h^2, \tau, H_0, \ln[10^{10} A_S], n_S, \sigma_8\}; \\
\sigma_{\text{Planck}} &= \{0.0003, 0.0029, 0.034, 1.29, 0.066, 0.01, 0.026\}; \\
\sigma_{\text{CORE}} &= \{0.00007, 0.0006, 0.004, 0.23, 0.008, 0.003, 0.002\};
\end{aligned}
\tag{3.2}$$

As already noticed in [26, 27], there is an improvement of almost an order of magnitude on the standard cosmological model constraints given by CORE with respect to Planck 2015. The improvement is mainly due to the better sensitivity in polarization and lensing measurements for CORE, although we need to bear in mind the differences between a real Planck likelihood including marginalization on nuisance parameters and the simplified ideal CORE likelihood where no residual foreground or systematic uncertainties, outside the instrumental error, are taken into account. Above and in the following, we also present the constraints for the Hubble parameter (H_0) today and σ_8 (in some of the cases), which are derived parameters. All the errors presented here represent 2σ confidence intervals.

3.4 Forecasts for primordial features

The results for the WWI models with Planck 2015 data, although in a slightly different form, were presented in [9]. In the following results we use the best fits of [9] as fiducial values for the CORE simulated data. Though in this paper we use a slightly modified form with respect to [9], note that since the latter is nested in the more general form used here the local best fits will not change; a simple change of variable translates the old best fit parameters to the modified parametrization.

| Parameter Constraints for WWI | | | | | |
|--|------------------------------------|------------------------------------|------------------------------------|------------------------------------|-----------------------------------|
| Parameters | WWI-A $\Delta_{\text{DOF}} = 4$ | WWI-B $\Delta_{\text{DOF}} = 4$ | WWI-C $\Delta_{\text{DOF}} = 4$ | WWI-D $\Delta_{\text{DOF}} = 4$ | WWI' $\Delta_{\text{DOF}} = 2$ |
| $\Omega_b h^2$ $\times 10^2$ | 2.217 ± 0.006 | 2.222 ± 0.006 | 2.217 ± 0.006 | 2.221 ± 0.006 | 2.218 ± 0.006 |
| $\Omega_{\text{CDM}} h^2$ $\times 10^2$ | 12.05 ± 0.06 | 12.03 ± 0.06 | 12.06 ± 0.06 | 12.04 ± 0.06 | 12.03 ± 0.06 |
| τ | 0.081 ± 0.005 | 0.093 ± 0.005 | $0.074^{+0.005}_{-0.004}$ | 0.092 ± 0.005 | 0.085 ± 0.005 |
| H_0 | 66.93 ± 0.25 | 67.06 ± 0.24 | $66.9^{+0.24}_{-0.23}$ | $67.03^{+0.25}_{-0.24}$ | 67.02 ± 0.23 |
| $\ln[10^{10} V_0]$ | 1.735 ± 0.009 | 1.754 ± 0.009 | $1.72^{+0.009}_{-0.008}$ | 1.757 ± 0.009 | 0.2809 ± 0.0009 |
| ϕ_0 | $0.013^{+0.008}_{-0.007}$ | $0.0037^{+0.0019}_{-0.0021}$ | 0.0057 ± 0.0022 | 0.003 ± 0.0005 | 0.1 ± 0.06 |
| γ | $0.03^{+0.04}_{<}$ | $0.041^{+0.035}_{<(-0.02)}$ | $0.026^{+0.028}_{<(-0.02)}$ | $0.034^{+0.02}_{-0.03}$ | - |
| ϕ_{T} | $7.887^{+0.012}_{-0.014}$ | $7.9104^{+0.0012}_{-0.0014}$ | $7.91^{+0.0016}_{-0.0017}$ | 7.9111 ± 0.0005 | $4.508^{+0.003}_{-0.002}$ |
| $\ln[\delta]$ | $-4.4^{+0.7}_{-0.8}$ | $-6.89^{+2.2}_{-1.3}$ | $-5.91^{+0.86}_{-0.73}$ | $10.2^{+1.6}_{<}$ | - |

Table 1. Background and inflationary parameter constraints WWI projected for CORE. For WWI potential we present the constraints on the parameters when CORE data is simulated using the four local best fits to the Planck data. For WWI' potential also we provide the constraints expected from CORE. Errors correspond to 95% confidence. For parameters that are unbounded at 2σ within the priors provided are denoted as $<$ (unbounded from below). If a value is quoted after $<$ in parenthesis, it implies the 68.3% error in that direction. Absence of error in parenthesis following $<$ denotes that the parameter is unbounded even in 1σ in that direction. The extra degrees of freedom compared to the strict slow-roll part inflation are provided by Δ_{DOF} .

In table 1, we list the constraints for CORE in the WWI case. We stress again that within the WWI potential, A, B, C, D represent the best fits that we obtained using Planck 2015 data in [9]. Since our objective is to predict at which significance level CORE data can constrain these favored models, should they be the real underlying model of the Universe, we have used the local best fits to the Planck TTTEEE + lowTEB + BKP datasets [†]. For the WWI' potential it generates one single class of features with only two parameters, this class improves the fit to both Planck temperature and polarization data compared to power law PPS. In the different rows of the table 1 we provide the background and inflationary parameter constraints, the columns represent the cases where WWI-A, B, C, D and WWI' best fits are used as fiducial cosmologies for our simulations.

[†]BKP represents joint likelihood from BICEP2-Keck array that includes dust polarization measurements from Planck [45]. We used the best fit parameters for this likelihood combination because of completeness. However, note that in this paper we are not using CORE BB likelihood.

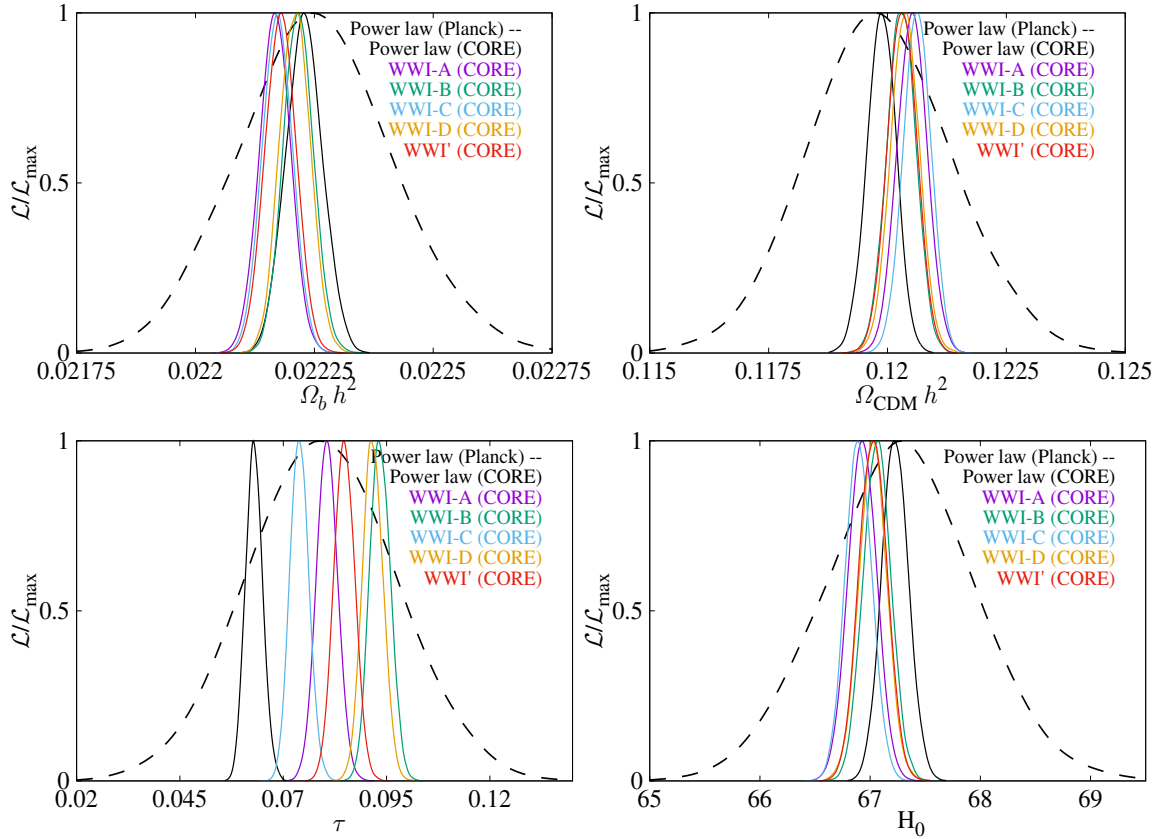


Figure 2. Background cosmological parameter constraints for power law and the WWI. For the power law, constraints obtained using Planck data are provided in dashed black and projected CORE constraints are provided in solid black. For the other cases, we just provide the results from CORE in solid line. A couple of points to note in these plots are: firstly, as expected, we obtain significant improvement in the constraints if we use simulated CORE sensitivity; secondly since each of the WWI local best fits from Planck is used for the CORE simulation as fiducial model, we find the likelihoods localized at different region in the background parameter space and for certain parameters, there are very little overlap between the likelihoods, indicating the ability to distinguish them in the future CMB observations.

Comparing the uncertainties in table 1 with those in 3.2 we note that though the PPS is characterized by more parameters, the WWI framework seems to constrain the baryon density comparably to the power law case. However, as has been discussed, in the WWI framework, we set the slow roll part of the potential (apart from the amplitude parameter, V_0) in a way that the spectral tilt generated in the featureless case is ~ 0.96 , in good agreement with Planck data. We are therefore reducing the space dimensionality of the standard cosmological parameters compared to the power law case.

It is however interesting to note that the presence of the features do not loosen the bounds on the cosmological parameters, except for τ . The reason for this is that WWI provides a power suppression on large scales for all its variants, hence the optical depths obtained in these models are all substantially different from the power law case, affecting the simulated CORE power spectra. Due to this degeneracy with the PPS shape, the constraints expected from CORE are slightly degraded.

In figure 2 we show the comparison of background parameters from power law and

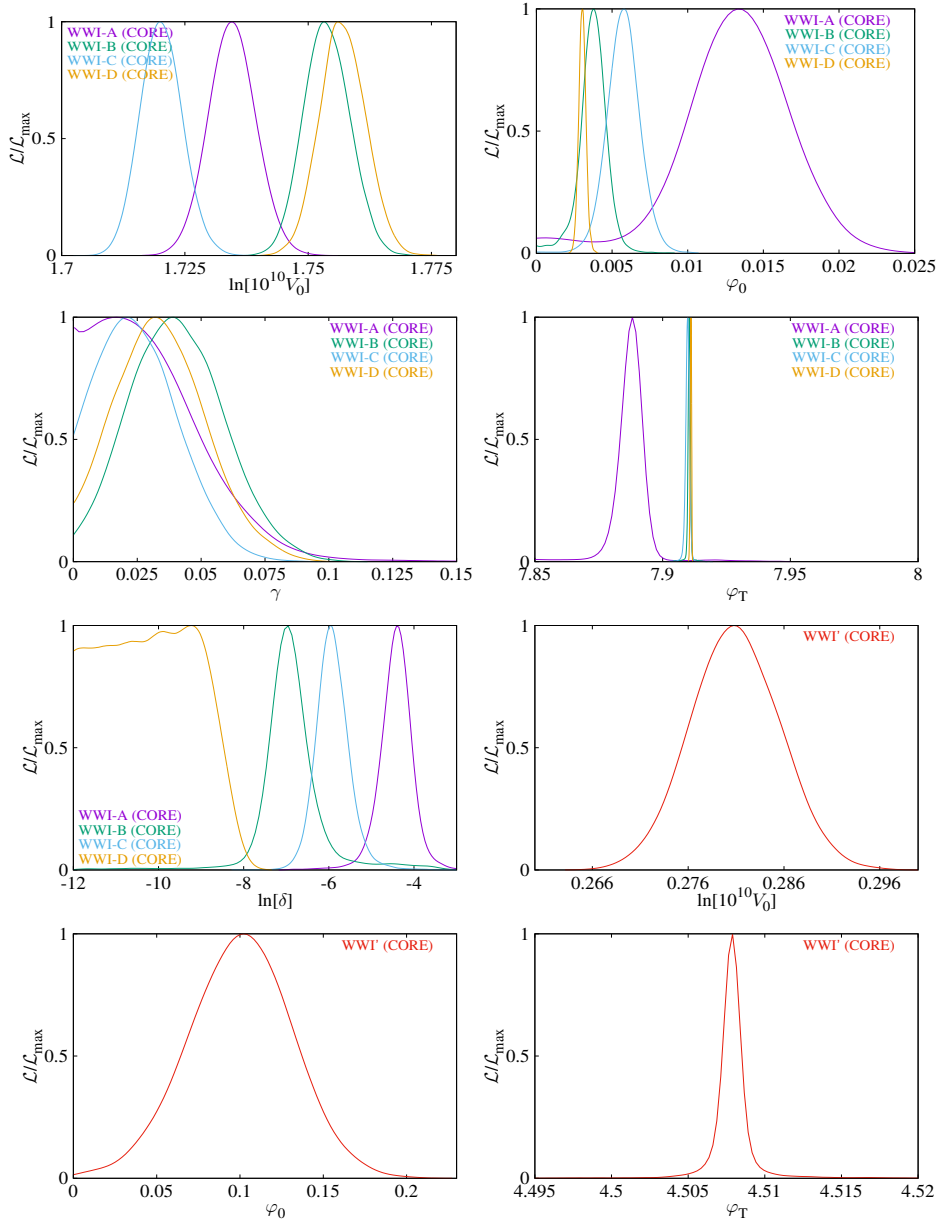


Figure 3. Constraints on inflationary potential parameters for WWI-[A,B,C,D] and WWI'. The first 5 plots from top with different posterior distributions correspond to WWI-[A,B,C,D] features and the last three single likelihoods represent WWI'. Note that for WWI potential, while Planck data can indicate different types of features as its local minima, these sets of plots are clearly showing that some of the features, should it represent the true model of the Universe, will be significantly detected with CORE. Wiggles in the WWI are characterized by ϕ_0 hence, the distance of $\phi_0 = 0$ from the maximum likelihood will dictate the significance of that type of wiggles with future data. The large scale suppression (generated by γ) will not be constrained well by future data owing to the cosmic variance. The amplitude of perturbations (controlled principally by V_0), however is constrained with high significance for all the models. Features continuing to small scales are found to have higher chances of being detected.

WWI. In order to highlight the present constraints, we plot also the Planck constraints on the concordance Λ CDM model in dashed black.

We stress that different features provide different best fits to the Planck 2015 and therefore in the CORE simulated data have different fiducial values for the cosmological parameters. The results show that while with Planck data all the different background parameter best fits fall within the uncertainties of the power law constraints, making it impossible to distinguish one from the other, with CORE it is possible not only to constrain some of the parameters which characterize the features but also distinguish among the different cosmological parameters associated with different features themselves increasing the possibility to distinguish among the possible models. For example, for baryon and CDM densities, the posterior peaks for WWI-A and C are quite off with respect to the power law. Most evidently we have differences for the optical depth, in fact, as discussed before, we find that τ from all the feature models can be distinguished. For the Hubble parameter we note a common trend as has been discussed in earlier papers [46–49]. The presence of any kinds of features, within the flexibilities of WWI framework, prefers a lower value of H_0 compared to power law.

Concerning the inflaton potential constraints we have five parameters for the WWI potential (four of which are the extra parameters to describe the beyond slow roll part) and three for WWI' potential (two extra parameter with respect to the canonical α -attractor case). Again all the bounds in table 1 are the 95% C.L. These constraints are extremely important in order to predict the probability of a specific feature model being detected in the future. Some parameters for the WWI, in particular γ and δ , remain partially unconstrained. The marginalized posteriors corresponding to these inflationary potential parameters are plotted in figure 3.

We note how the scale of inflation V_0 will be tightly constrained by an instrument like CORE, as it fixes the overall CMB normalization scale. The parameter ϕ_0 denotes the amplitude of primordial oscillations as it determines the height of discontinuities in the potential (for WWI potential) or in its derivative (for WWI' potential). Hence, the greater is the distance of $\phi_0 = 0$ from the peak of the posterior the higher is the confidence to rule out the power law model, assuming that the corresponding inflationary feature represents the true model of the Universe. The results show how with an experiment like CORE it would be possible to detect the features chosen within the WWI framework, from moderate to high significance, should they represent the real Universe [‡]. For example WWI-A and WWI-B features are constrained to 2-3 σ level, WWI-C and WWI' have $\sim 3\sigma$ significance. WWI-D, where oscillations extend to small scales (all the scales probed by CORE), has the highest probability of being detected ($\gg 3\sigma$) due to its small scale signature which is in the optimal range of CORE.

The extent of large scale suppression in these models, controlled by γ , however, is not strongly constrained in any of the features from WWI potential, even with a sensitivity and a sky coverage of an instrument like CORE, mainly due to cosmic variance. Of these suppression, WWI-B which has the largest suppression amongst all the PPS, obviously has the best probability ($\sim 2\sigma$) as can be noted from table 1.

The parameter ϕ_T is related to the location of the feature. Its constraints indicate at which scale particular feature is favored by the data and that translates exactly to the field value of the phase transition during inflation. Note that the feature positions in all the cases are well constrained. However, the variance in the position from WWI-A is largest as it represents the largest scale feature and a small shift in the feature position do not significantly degrade the likelihood.

[‡]We define moderate significance by $< 3\sigma$ C.L.

The width of the step, that defines the sharpness of the wiggles, is also an indicator for the evidence of the features. Different types of features are classified also by the characteristic frequency of the oscillations, the constraints on the $\ln[\delta]$ in WWI potential show posterior distributions with peaks localized in four different regions in the parameter space opening the possibility to distinguish among different models also through this parameter. The width in WWI-A, B, C and WWI' are well constrained whereas for WWI-D we have an upper bound which shows that steps sharper than $\ln[\delta] \sim -10$ will not be constrained.

4 Reionization history

Einstein-Boltzmann codes, such as CAMB [50, 51], typically use a fixed form to model the reionization history, namely it is assumed that the free electron fraction follows a hyperbolic tangent in the following form:

$$x_e(z) = \frac{1 + F_{\text{He}}}{2} \left[1 + \tanh \left(\frac{y(z_{\text{re}}) - y(z)}{\delta_{\text{Reion}}} \right) \right], \quad (4.1)$$

where, $y(z) = (1+z)^{3/2}$. $\delta_{\text{Reion}} = 1.5\sqrt{1+z_{\text{re}}}dz$ where dz is fixed to be 0.5 in Planck baseline analysis. $x_e(z)$ is the free electron fraction *w.r.t.* hydrogen, the factor $1 + F_{\text{He}}$ accounts for the corrections due to the fraction of Helium and F_{He} in this treatment is derived consistently with Big Bang Nucleosynthesis and it approximately takes the value 0.08. In addition, at a redshift of 3.5, considering doubly ionized Helium, another Tanh step for Helium with an asymptotic factor of F_{He} is added to the electron fraction. z_{re} denotes the redshift where the free electron fraction from hydrogen is 0.5. Defining the reionization history in this way, CAMB does a search in the z_{re} and find the redshift of reionization for a given optical depth τ which is one of the baseline parameter in the Markov-Chain Monte Carlo analysis code COSMOMC [52, 53].

In order to allow for more freedom in the reionization history, and be compatible with current observations, we use a model characterized by one additional parameter (hereafter addressed as Poly-Reion) defined as:

$$x_e(z) = (1 + F_{\text{He}})f(z), \quad (4.2)$$

where $f(z)$ is a polynomial. $f(z)$ is a Piecewise Cubic Hermite Interpolating Polynomial (PCHIP). The polynomial is determined by the electron fraction at four redshifts (the nodes in the polynomial): $z = 0, 5.5, 7$ and $z_{xe=0}$. From the observations we have $f(z = 0) = f(z = 5.5) = 1$ [54] conservatively [§], thereby we are excluding too much late reionizations. $f(z = 7) = x_e(z = 7)$ is a free parameter, where the choice of a node at $z = 7$ is well justified by the observed presence of neutral hydrogen at different lines of sight using Quasar and Gamma Ray Burst data [55]. $z_{xe=0}$ defines the epoch in the past where the Universe was fully neutral and it is fixed by solving for the given optical depth:

$$\tau = \int \sigma_{\text{T}} n_e(z) dl, \quad (4.3)$$

[§]The authors report neutral hydrogen fraction to be 10^{-4} at $z < 5.5$. At the same time since they find a sharp increase in neutral hydrogen up to 0.1 by redshift 6, using this Poly-Reion method we will be allowing such scenarios with some neutral hydrogen before $z = 5.5$.

where, $n_e(z)$ is the free electron density and σ_T is the Thomson scattering cross section. The $f(z)$ can never be greater than 1 or less than 0 and respects a monotonic increase in free electron density from past to present. Using the f_z 's at the given nodes, PCHIP ensures the monotonicity of $x_e(z)$. The Poly-Reion model has three main advantages with respect to the step model:

- it is by construction in agreement with observations of a fully ionized medium at $z = 5.5$;
- it allows more freedom being characterized by the free parameter $f(z = 7) = x_e(z = 7)$;
- it naturally provides the redshift where reionization started as a derived parameter.

Unlike the Tanh model, the Poly-Reion does not lead to symmetric reionization histories. Although there may be significant overlaps in the reionization histories they model, the Tanh-Reion parametrization is not nested within the Poly-Reion model. The Poly-Reion is also different from the asymmetric reionization history analyzed with Planck data in [56] and in the perspective of the CORE concept in [26]. Note that in a recent paper, two of us have discussed a Poly-Reion form of reionization history [57]. The model discussed here is nested within that generic model.

4.1 Solving for reionization

The Poly-Reion reionization history has an extra parameter $x_e(z = 7)$ in addition to τ , which is the only free parameter for Tanh-Reion. The earliest redshift that is used for the polynomial is $z_{xe=0}$ and we require $f(z) = 0$ (for all $z \geq z_{xe=0}$) such that the Universe is fully neutral before that redshift. We do a search from $z = 7.25$ (we use this value instead of 7 to avoid sharp step for CAMB integrals) and the maximum redshift for the onset of reionization (we assume $z_{\max} = 70$) that matches the τ provided. $x_e(z = 7)$ is varied between 0 to 1, the values in this range which cannot solve for the values of τ are rejected.

First we derive the constraints for the Planck 2015 data. We use the public available low and high- ℓ likelihood Planck 2015 TTTEEE + lowTEB + lensing. The Planck lensing likelihood lowers the value of the optical depth, using Tanh-reion, to $\tau = 0.063 \pm 0.014$, which is closer to the most recent value reported in Planck 2016 Intermediate paper with $\tau = 0.0596 \pm 0.0089$ [58]. We use the mean values as fiducial parameters for the CORE simulated data.

4.2 Constraints on Reionization history

As already been mentioned, the Tanh-Reion is not nested within the more general Poly-Reion. However, since we aim to propose Poly-Reion as an alternative model for reionization history, we will present and discuss the results of the constraints on cosmological parameters using the two models.

The best fit $-2 \ln \mathcal{L}$ obtained from Powell's BOBYQA method [¶] for Planck TTTEEE + lowTEB + lensing when Tanh-Reion is used is 12947.2. For Poly-Reion we find $-2 \ln \mathcal{L}_{\max} = 12944.6$. Hence we find roughly an improvement of 2.6, with an extra parameter, compared to the Tanh reionization histories. In table 2 we provide the bounds on the cosmological parameters when Poly-Reion is used for the reionization history for both Planck real data and CORE forecasts. Instead of presenting the results for $z_{xe=0}$ we prefer to use the duration

[¶]In order to obtain the best fits we use Powell's BOBYQA (Bound Optimization BY Quadratic Approximation) method of iterative minimization [59].

| Parameter Constraints for Poly-Reion | | |
|---------------------------------------|---------------------------|-----------------------------|
| Parameters | Planck | CORE |
| $\Omega_b h^2 \times 10^2$ | 2.23 ± 0.03 | 2.228 ± 0.007 |
| $\Omega_{\text{CDM}} h^2 \times 10^2$ | $11.89^{+0.26}_{-0.27}$ | $11.885^{+0.054}_{-0.055}$ |
| τ | 0.069 ± 0.025 | 0.0696 ± 0.0044 |
| $x_e(z = 7)$ | $0.45^{+0.49}_{-0.37}$ | $0.53^{+0.33}_{-0.29}$ |
| H_0 | $67.65^{+1.23}_{-1.18}$ | $67.68^{+0.23}_{-0.22}$ |
| $\ln[10^{10} A_S]$ | $3.07^{+0.047}_{-0.046}$ | $3.071^{+0.0076}_{-0.0074}$ |
| n_S | 0.966 ± 0.009 | 0.9661 ± 0.0029 |
| Δ_z^{Reion} | $8.2^{+7.2}_{-7.3}$ | $8.5^{+2.2}_{-3.1}$ |
| z_{re} | $7.25^{+2.4}_{-1.3}$ | $7.46^{+1.86}_{-1.34}$ |
| σ_8 | $0.818^{+0.017}_{-0.016}$ | 0.819 ± 0.002 |

Table 2. Present and projected constraints on reionization history (and other background and perturbation parameters) assuming Poly-Reion, using Planck data and CORE simulated data respectively. Errors correspond to 95% C. L. A comparison with Planck results in [1] indicates that apart from the optical depth, all other parameters have similar constraints.

of reionization Δ_z^{Reion} which is defined as the difference between the redshift when the reionization is 10% complete and the redshift when it is 99% complete. This parameter is in fact much better constrained by both Planck and CORE with a much better behaved distribution compared to $z_{x_e=0}$. Note that this duration of reionization is different from the δ_{Reion} used in Eq. 4.1.

We note by comparing the results in table 2 and the Planck results [1] that the constraints on background and power law PPS parameters do not change much for Tanh-Reion and Poly-Reion, instead the mean values for τ and A_S are shifted due to degeneracies. We present also the two derived parameters: z_{re} which represents the redshift where the electron fraction from hydrogen is exactly half and Δ_z^{Reion} which is duration of reionization. In figure 4 we present the comparison of the reionization histories from Planck and the forecasts for CORE. In order to display the correlation, we provide the 2D marginalized contours for $x_e(z = 7)$ and Δ_z^{Reion} at the bottom panel of the same figure. The dependence on τ is represented by the rainbow colormap of the points.

For a given electron fraction, to solve Eq. 4.3 for increasing value of optical depth, we need to increase the total duration of reionization period and thereby we require higher (earlier) value for $z_{x_e=0}$. To show the different reionization histories given by this model we have randomly selected from the samples within 1σ and between $1 - 2\sigma$ contours and we plot the electron fraction (not considering Helium reionization) for the entire reionization histories for Planck and CORE bounds in figure 5 in the redshift range 0–55. For comparison the best fit of Tanh-Reion is plotted in dashed black. Since samples from different confidence limits will intersect each other in redshifts, we plot the samples rather than providing confidence bands. Within the chosen fiducial models we note how Planck constraint is limited to the range $5.5 < z < 50$ (the lower limit being prior dominated) CORE can reduce the range to $5.5 < z < 25$. Though this constraint is strictly dependent on the chosen fiducial reionization

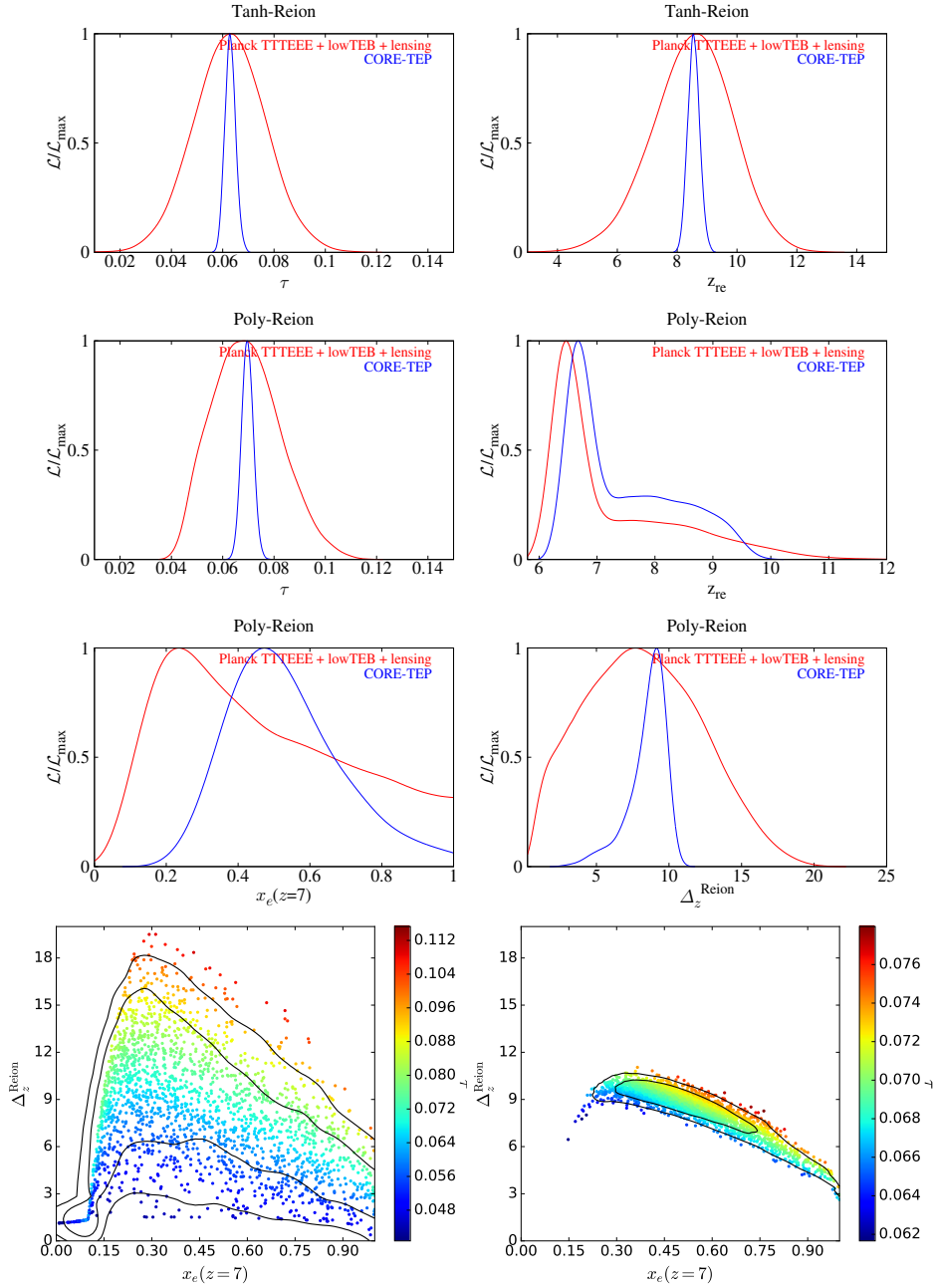


Figure 4. Current constraints on the reionization history and the forecasts for CORE. First three rows from the top represent the constraints from Planck TTTEEE+lowTEB+lensing in red and the projected CORE constraints in blue. In the topmost panel we have plotted the optical depth (τ) and the reionization redshift (z_{re}) for the Tanh model of reionization histories. The rest of the rows represent Poly-Reion scenario. Two middle rows plot the marginalized probability distribution of τ , z_{re} , $x_e(z=7)$ and reionization duration Δ_z^{Reion} respectively (in order of reading from left to right and top to bottom). The plots at the bottom most panel show the correlation between history parameters $x_e(z=7)$ and Δ_z^{Reion} . The left plot shows the Planck bounds and the right plot predicts the CORE constraints. Note that, as expected, CORE predictions give significantly tighter constraints on the history of reionization.

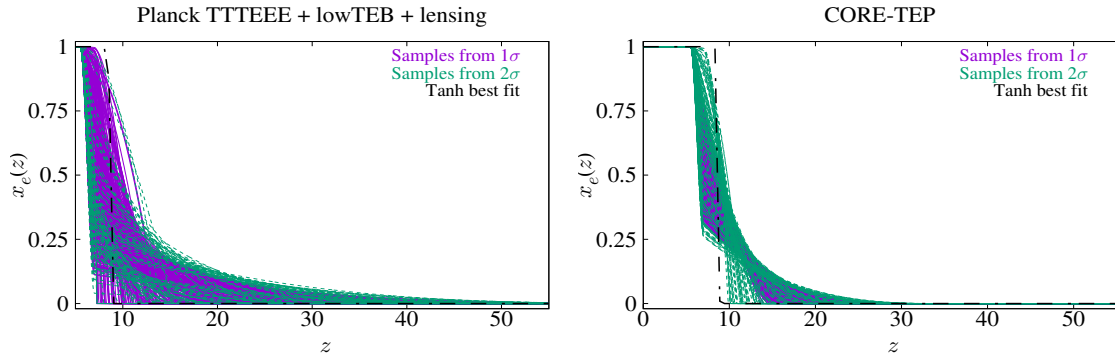


Figure 5. Free electron fraction (not including electrons from singly and doubly ionized Helium, while in the analysis we have included both) as a function of redshift. The samples are plotted for the actual Planck (left) dataset and the simulated CORE (right) dataset. Samples from 1σ confidence are plotted in solid and 2σ samples are plotted in dashed lines. Needless to mention, these lines integrate to provide different values of the optical depth. We have plotted samples instead of bands on the electron fraction as some of the features and the flexibility of the model are better seen in sample representation. In black dash-dotted line, we have plotted the best fit Tanh-Reionization history obtained with Planck TTTEEE + lowTEB + lensing.

history, the improvement due to the better noise sensitivity in CORE is quite evident. By comparing table 2 and Eq. 3.2, we see that τ uncertainty does not degrade significantly at CORE sensitivity by allowing more freedom in the reionization history, as was already noticed in [26] for a different asymmetric reionization history.

We note how although Tanh-Reion and Poly-Reion both provide very similar fits to the data, they have very different reionization histories, allowing also for mutually exclusive results. In both plots, the Poly-Reion $1-2\sigma$ samples extend to the direction of lower electron densities at low- z and thereby demand a higher value for the beginning redshift of reionization. This signifies that there are hints and possibilities of extended reionization. A free-form reionization history parametrization as in [57] will be more effective in the future in understanding the redshift-dependent constraints of the free electron fractions and that will allow complicated models relaxing these bounds to a certain extent.

5 Confusion between inflationary features and extended reionization history

We now discuss to what extent an extended reionization scenario such as Poly-reion can be partially degenerate in generating similar polarization anisotropy as the large-scale inflationary features in the PPS produce. In order to assess this degeneracy, we use the following approach. WWI-A, amongst all the best fits, generates a suppression and large-scale oscillation and thereby provides the improvement in fit to the TT data. Though the large-scale polarization data at hand can not support or deny this feature, we assume WWI-A to be the fiducial model of the Universe. We present directly the forecasts for CORE, that with its good polarization sensitivity may target this issue. Being characterized by one extra parameter, while Poly-Reion is not expected to provide sufficient flexibility to mimic the polarization features from WWI-A, it can produce a variety of extended reionization

histories. For completeness we use the TT, TE and EE data together even if Poly-Reion is expected to affect mainly the large scale polarization.

To investigate the possible confusion caused by this degeneracy, we study how the fit to the data where the fiducial is given by the WWI-A is improved when using a power law PPS (hence not the real PPS model of the Universe we are assuming) with Poly-Reion instead of Tanh-Reion. In this way we may asses if the use of Poly-Reion model may lead to a better fit with a power law PPS though the real Universe is represented by a WWI-A cosmology reducing the possibility to detect such a model in more free reionization histories.

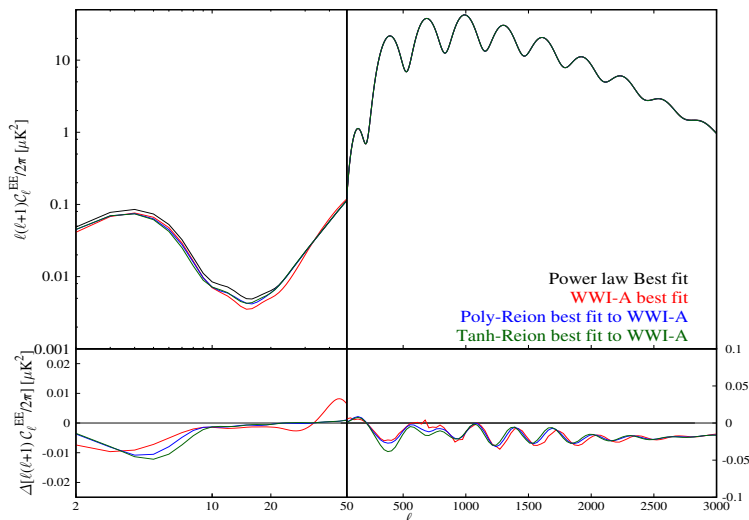


Figure 6. Polarization angular power spectra for different models. The angular power spectrum are plotted for the best fit Planck results for power law and WWI-A. For the Tanh-reion and Poly-reion, the plotted power spectra represent the best fit to the simulated WWI-A spectrum for CORE. The bottom inset plot represent the differences in the angular power spectra *w.r.t* the power law best fit. Note that though the Poly-reion does not have much flexibilities that can address the inflationary features in the polarization data, in both TE and EE spectra, it performs better than the Tanh-reion, owing to its one extra parameter.

We compare the difference in average likelihoods between the power law model with Tanh-Reion and Poly-Reion compared to WWI-A model with Tanh-Reion. We simulate CORE spectra with best fit WWI-A feature and Tanh-Reion. We derive the $\chi^2 = -2 \ln \mathcal{L}$ for (i) the WWI-A with Tanh-Reion, (ii) power law PPS with Tanh-Reion and (iii) power law PPS with Poly-Reion all to fit WWI-A simulated spectra. We then compare the average χ^2 within 1-10% of the maximum likelihood values. We find, if we use Poly-Reion model with power law, it can fit the WWI-A feature 6-9% better (in χ^2) compared to Tanh-Reion case. Therefore we can confirm the Poly-Reion introduces features in reionization history that can mimic parts of the WWI-A feature to a limited extent.

In the figure 6, we plot the differences between (i),(ii) and (iii) in the EE anisotropy power spectra. The best fit spectra for power law and Tanh-Reion and from (i),(ii) and (iii) are plotted in black, red, green and blue respectively. In the inset, we plot the differences between different runs and the power law best fit spectra. Note that in both EE and TE spectra,(iii) is closer to (i) compared to (ii) at large scales. At smaller scales the changes are due to difference in the best fit background cosmological parameters.

To investigate further the extent of the confusion, we attempt to fit WWI-A fiducial

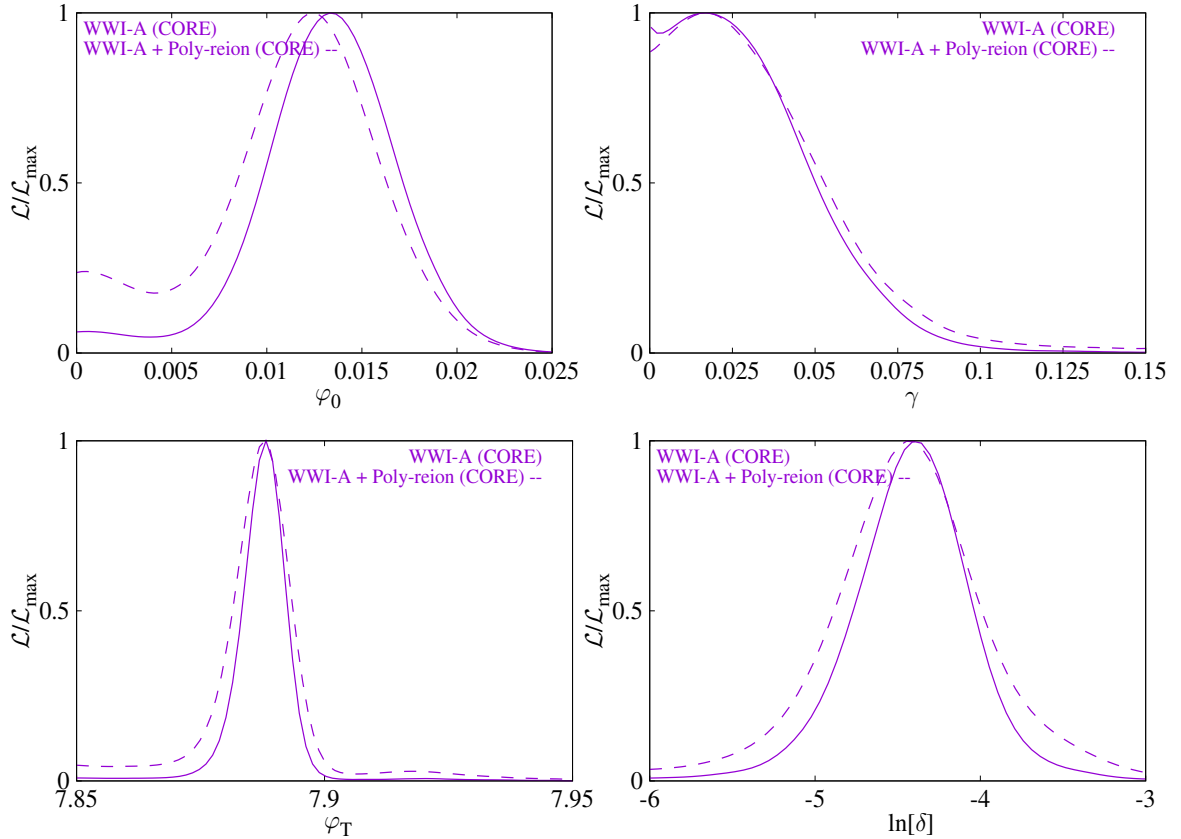


Figure 7. Shifts in the inflationary potential parameters when Poly-reion is used as model for reionization instead of Tanh-reion. We have used WWI-A as fiducial model as this best fit has features only at largest scales. We note that the parameter ϕ_0 which is moderately constrained ($2 - 3\sigma$) in the Tanh-reion scenario, is now constrained with slightly less significance ($1 - 2\sigma$). Negligible change in the parameter responsible for large scale suppression (γ) is noticed. Since the position (ϕ_T) and the width (δ) of the discontinuity is related with the extent of discontinuity (ϕ_0), we notice change in these parameters as well. The changes in the background parameter constraints are negligible and therefore not presented.

with WWI model combined with Poly-reion scenario. Here we use temperature, polarization and lensing likelihood similar to what we have considered in section 3. We compare the obtained marginalized likelihoods of the inflationary feature parameters (ϕ_0, γ, ϕ_T and $\ln[\delta]$) with the likelihoods from section 3) in figure 7. We compare the cases where WWI-A is used as fiducial. Note that we do not find significant change in the posteriors. Definitely the significance of the feature has been reduced as for ϕ_0 posterior has shifted closer to *zero*. We find that the previously obtained moderate significance $2\sigma - 3\sigma$ reduces to $1\sigma - 2\sigma$ when we use Poly-reion. This decrease in significance is partially caused by the extended reionization that can generate parts of the WWI-A feature in the polarization anisotropy. We find no noticeable change in the background parameters.

This study of confusion here indicates that an extended reionization history will not restrict our capabilities of finding large scale features to significant extent with the future surveys having the sensitivity of CORE. We have used more nodes in the Poly-reion parametrization between $7 < z < 70$ to allow more complex reionization histories, how-

ever, we do not find notable increase in degeneracy between the reionization history and the WWI-A. Therefore we can further comment that given a realistic reionization history with $0 < x_e(z) < 1$ and monotonic increase of x_e with the decrease in redshifts, the degeneracy between large scale inflationary features and the process of reionization is limited.

6 Conclusions

In this paper, we address three important aspects of cosmological parameter estimation with next generation space based CMB surveys, namely, features in the primordial power spectra, non-instantaneous reionization histories and the possible degeneracies between these two aspects. For the first part, to avoid the use of different models of features, we use the more general Wiggly Whipped Inflation that provides different feature models within the same framework. WWI includes inflationary phase transitions with discontinuities in potential or in its derivative. In our earlier analysis [9], we had demonstrated that using only one potential with 2-4 extra parameters, we can generate multitudes of inflationary features that are discussed in literature using different potentials. The advantage of using WWI is that with the same potential or same framework we can locate the existence of features that are supported by the data in one step.

Using Planck 2015 temperature and polarization data, from WWI framework we identified 5 distinct features that improve the fit to the Planck data, although not at a statistical significance level, with respect to the power law form of the PPS: WWI-[A, B, C, D] and WWI'. WWI-[A, B, C, D] come from the same potential with a discontinuity whereas WWI' is from another potential with discontinuity in the derivative. All the PPS considered here contain suppression on large angular scales then we have that: WWI-A contains localized wiggles in the PPS at scales corresponding to $\ell = 20 - 40$; WWI-B, C and WWI' introduce oscillations which are extended towards smaller scales compared to WWI-A; WWI-D contains non-local oscillations that continue up to smallest angular scales (up to the observational limit assumed in this paper).

In this paper we addressed the possibility that future space CMB observations will detect features in the inflaton potential if they represent the true model of the Early Universe. We take CORE as an example for a future CMB space satellite concept and we tested WWI framework against simulated data for temperature, polarization and lensing potential. The results show that broadly we have a moderate significance to features in the inflaton potential leading to features in the primordial power spectrum that are localized to certain cosmological scales. While for WWI-A and WWI-B, we find $2 - 3\sigma$ significance of rejection of featureless PPS, wiggles in WWI-C and WWI' show just 3σ C.L. WWI-D on the other hand has highest probability of detection where the amplitude of wiggles reject *zero* amplitude at much more than 3σ . Since WWI-D has oscillations continuing to small scales, CORE is expected to capture its fine oscillations at high significance with better small scale measurements. In all the cases we find $< 2\sigma$ significance for the suppression at large scale primordial power since cosmic variance is expected to limit our ability to detect such large scale signals ^{||}.

^{||}However, we must mention that, here we are only considering the local best fits to the Planck 2015 data obtained in the WWI framework. It is entirely possible that even within this framework there are wide features with higher amplitude that are still allowed by the Planck data and which would be probed at higher significance with CORE. Our analysis does not rule out such possibilities.

We have observed a consistent reduction of the capability of future CMB polarization data to probe features at large scales with respect to previous literature, as also noticed in [60]. The degraded significance of the feature generated by a step in the potential (similar to WWI-A) as compared to [31] can be attributed to two facts. In this paper we use CORE noise sensitivity rather a cosmic variance ideal experiment as in [31]. Secondly, wiggles in WWI-A are 22% lower in amplitude compared to best fit potential-step-like feature obtained in WMAP. Although the Planck measurements have somewhat reduced the suggestion of large scale features, the combination of data from future galaxy surveys with CMB observations is an interesting avenue to probe the primordial origin of the deviations from the Λ CDM best-fit in Planck temperature data [60].

To probe extended reionization histories, we use a Piecewise Cubic Hermite Interpolating Polynomial to model the free electron fraction as a function of redshift. This is a more economic extension of the instantaneous reionization history than the PCA [32] approach which might be useful given the decrement in the value of the optical depth with Planck [2, 58]. Assuming completion of hydrogen reionization by $z < 5.5$, in agreement with current astrophysical observations, and a monotonic decrease of the electron fraction, we confront this model against Planck 2015 data with one extra parameter compared to the Tanh-Reion case. Although Poly-Reion does not encompass the Tanh-Reion for all optical depth values, we find marginal improvement in fit compared to the standard case. In this parametrization we could constrain the duration of reionization (redshifts between 10% to 99% reionization) within 1 to 15 redshifts with Planck data at 2σ C.L. CORE spectra is expected to improve the constrain three times compared to Planck data.

Apart from proposing Poly-Reion as suitable extended reionization model, we also make use of it in exploring the possible confusion between primordial features and reionization histories. Although this monotonic reionization history is not able to reproduce the primordial features in polarization to a great extent, we show that large scale suppression from WWI-A can be slightly obscured by the presence of the reionization history. The significance of feature when WWI-A is used as fiducial spectra, decrease from $2 - 3\sigma$ to $1 - 2\sigma$ if Poly-reion is used as the model of reionization. Further investigations show that a more complex but realistic and monotonic reionization history can not create much confusion with the inflationary features given CORE sensitivity where temperature, polarization and lensing likelihoods are used for parameter constraints.

Acknowledgments

The authors would like to acknowledge the use of APC cluster (<https://www.apc.univ-paris7.fr/FACeWiki/pmwiki.php?n=Apc-cluster.Apc-cluster>). DKH and GFS acknowledge Laboratoire APC-PCCP, Université Paris Diderot and Sorbonne Paris Cité (DXCACHEXGS) and also the financial support of the UnivEarthS Labex program at Sorbonne Paris Cité (ANR-10-LABX-0023 and ANR-11-IDEX-0005-02). DP, MB and FF acknowledge financial support by ASI Grant 2016-24-H.0 and partial financial support by the ASI/INAF Agreement I/072/09/0 for the Planck LFI Activity of Phase E2. MB acknowledge the support from the South African SKA Project. AS would like to acknowledge the support of the National Research Foundation of Korea (NRF-2016R1C1B2016478). AAS was partially supported by the grant RFBR 17-02-01008 and by the Russian Government Program of Competitive Growth of Kazan Federal University.

References

- [1] P. A. R. Ade *et al.* [Planck Collaboration], arXiv:1502.01589 [astro-ph.CO].
- [2] N. Aghanim *et al.* [Planck Collaboration], [arXiv:1507.02704 [astro-ph.CO]].
- [3] P. A. R. Ade *et al.* [Planck Collaboration], arXiv:1502.02114 [astro-ph.CO].
- [4] P. A. R. Ade *et al.* [Planck Collaboration], arXiv:1502.01592 [astro-ph.CO].
- [5] P. A. R. Ade *et al.* [Planck Collaboration], *Astron. Astrophys.* **571** (2014) A22 doi:10.1051/0004-6361/201321569 [arXiv:1303.5082 [astro-ph.CO]].
- [6] D. K. Hazra, A. Shafieloo and T. Souradeep, *JCAP* **1411**, no. 11, 011 (2014) doi:10.1088/1475-7516/2014/11/011 [arXiv:1406.4827 [astro-ph.CO]].
- [7] D. K. Hazra, A. Shafieloo and G. F. Smoot, *JCAP* **1312**, 035 (2013) arXiv:1310.3038 [astro-ph.CO].
- [8] D. K. Hazra, A. Shafieloo, G. F. Smoot and A. A. Starobinsky, *JCAP* **1408**, 048 (2014) doi:10.1088/1475-7516/2014/08/048 [arXiv:1405.2012 [astro-ph.CO]].
- [9] D. K. Hazra, A. Shafieloo, G. F. Smoot and A. A. Starobinsky, *JCAP* **1609**, no. 09, 009 (2016) doi:10.1088/1475-7516/2016/09/009 [arXiv:1605.02106 [astro-ph.CO]].
- [10] R. Kallosh and A. Linde, *JCAP* **1307**, 002 (2013) doi:10.1088/1475-7516/2013/07/002 [arXiv:1306.5220 [hep-th]]; R. Kallosh and A. Linde, *JCAP* **1312**, 006 (2013) doi:10.1088/1475-7516/2013/12/006 [arXiv:1309.2015 [hep-th]]; R. Kallosh, A. Linde and D. Roest, *JHEP* **1311**, 198 (2013) doi:10.1007/JHEP11(2013)198 [arXiv:1311.0472 [hep-th]].
- [11] A. A. Starobinsky, *Phys. Lett. B* **91**, 99 (1980). doi:10.1016/0370-2693(80)90670-X
- [12] A. A. Starobinsky, *JETP Lett.* **55**, 489 (1992).
- [13] J. A. Adams, B. Cresswell and R. Easther, *Phys. Rev. D* **64** (2001) 123514 [astro-ph/0102236]; L. Covi, J. Hamann, A. Melchiorri, A. Slosar and I. Sorbera, *Phys. Rev. D* **74** (2006) 083509 [astro-ph/0606452]; V. Miranda, W. Hu and P. Adshead, *Phys. Rev. D* **86**, 063529 (2012) [arXiv:1207.2186 [astro-ph.CO]]; M. Benetti, arXiv:1308.6406 [astro-ph.CO]; A. E. Romano and A. G. Cadavid, arXiv:1404.2985 [astro-ph.CO]; J. Chluba, J. Hamann and S. P. Patil, *Int. J. Mod. Phys. D* **24** (2015) no.10, 1530023 doi:10.1142/S0218271815300232 [arXiv:1505.01834 [astro-ph.CO]].
- [14] D. K. Hazra, M. Aich, R. K. Jain, L. Sriramkumar and T. Souradeep, *JCAP* **1010**, 008 (2010) [arXiv:1005.2175 [astro-ph.CO]].
- [15] A. Ashoorioon and A. Krause, hep-th/0607001; T. Biswas, A. Mazumdar and A. Shafieloo, *Phys. Rev. D* **82**, 123517 (2010) [arXiv:1003.3206 [hep-th]]; R. Flauger, L. McAllister, E. Pajer, A. Westphal and G. Xu, *JCAP* **1006**, 009 (2010) [arXiv:0907.2916 [hep-th]]; C. Pahun, M. Kamionkowski and A. R. Liddle, *Phys. Rev. D* **79**, 083503 (2009) doi:10.1103/PhysRevD.79.083503 [arXiv:0807.0322 [astro-ph]]; M. Aich, D. K. Hazra, L. Sriramkumar and T. Souradeep, *Phys. Rev. D* **87**, 083526 (2013) [arXiv:1106.2798 [astro-ph.CO]]; D. K. Hazra, *JCAP* **1303**, 003 (2013) [arXiv:1210.7170 [astro-ph.CO]]; H. Peiris, R. Easther and R. Flauger, arXiv:1303.2616 [astro-ph.CO]; P. D. Meerburg and D. N. Spergel, *Phys. Rev. D* **89**, 063537 (2014) [arXiv:1308.3705 [astro-ph.CO]]; R. Easther and R. Flauger, arXiv:1308.3736 [astro-ph.CO]; H. Motohashi and W. Hu, *Phys. Rev. D* **92**, no. 4, 043501 (2015) doi:10.1103/PhysRevD.92.043501 [arXiv:1503.04810 [astro-ph.CO]]; V. Miranda, W. Hu, C. He and H. Motohashi, *Phys. Rev. D* **93**, no. 2, 023504 (2016) doi:10.1103/PhysRevD.93.023504 [arXiv:1510.07580 [astro-ph.CO]].
- [16] R. Allahverdi, K. Enqvist, J. Garcia-Bellido and A. Mazumdar, *Phys. Rev. Lett.* **97** (2006) 191304 [hep-ph/0605035]; R. K. Jain, P. Chingangbam, J. -O. Gong, L. Sriramkumar and T. Souradeep, *JCAP* **0901** (2009) 009 [arXiv:0809.3915 [astro-ph]].

- [17] A. Achcarro, V. Atal, P. Ortiz and J. Torrado, Phys. Rev. D **89**, no. 10, 103006 (2014) doi:10.1103/PhysRevD.89.103006 [arXiv:1311.2552 [astro-ph.CO]].
- [18] S. Hannestad, Phys. Rev. D **63** (2001) 043009 [astro-ph/0009296]; M. Tegmark and M. Zaldarriaga, Phys. Rev. D **66** (2002) 103508 [astro-ph/0207047]; S. L. Bridle, A. M. Lewis, J. Weller and G. Efstathiou, Mon. Not. Roy. Astron. Soc. **342** (2003) L72 [astro-ph/0302306]; P. Mukherjee and Y. Wang, Astrophys. J. **599** (2003) 1 [astro-ph/0303211]; D. Tocchini-Valentini, Y. Hoffman and J. Silk, Mon. Not. Roy. Astron. Soc. **367** (2006) 1095 [astro-ph/0509478]; A. Shafieloo and T. Souradeep, Phys. Rev. D **70** (2004) 043523 [astro-ph/0312174]; N. Kogo, M. Sasaki and J. 'i. Yokoyama, Prog. Theor. Phys. **114** (2005) 555 [astro-ph/0504471]; S. M. Leach, Mon. Not. Roy. Astron. Soc. **372** (2006) 646 [astro-ph/0506390]; A. Shafieloo and T. Souradeep, Phys. Rev. D **78** (2008) 023511 [arXiv:0709.1944 [astro-ph]]; P. Paykari and A. H. Jaffe, Astrophys. J. **711** (2010) 1 [arXiv:0902.4399 [astro-ph.CO]]; G. Nicholson and C. R. Contaldi, JCAP **0907**, 011 (2009) [arXiv:0903.1106 [astro-ph.CO]]; C. Gauthier and M. Bucher, JCAP **1210**, 050 (2012) [arXiv:1209.2147 [astro-ph.CO]]; R. Hlozek, J. Dunkley, G. Addison, J. W. Appel, J. R. Bond, C. S. Carvalho, S. Das and M. Devlin *et al.*, Astrophys. J. **749** (2012) 90 [arXiv:1105.4887 [astro-ph.CO]]; J. A. Vazquez, M. Bridges, M. P. Hobson and A. N. Lasenby, JCAP **1206**, 006 (2012) [arXiv:1203.1252 [astro-ph.CO]]; D. K. Hazra, A. Shafieloo and T. Souradeep, JCAP **1307**, 031 (2013) [arXiv:1303.4143 [astro-ph.CO]]; P. Hunt and S. Sarkar, arXiv:1308.2317 [astro-ph.CO]; S. Dorn, E. Ramirez, K. E. Kunze, S. Hofmann and T. A. Ensslin, JCAP **1406**, 048 (2014) [arXiv:1403.5067 [astro-ph.CO]]; D. K. Hazra, A. Shafieloo, G. F. Smoot and A. A. Starobinsky, JCAP **1406**, 061 (2014) doi:10.1088/1475-7516/2014/06/061 [arXiv:1403.7786 [astro-ph.CO]].
- [19] H. V. Peiris *et al.* [WMAP Collaboration], Astrophys. J. Suppl. **148**, 213 (2003) [astro-ph/0302225].
- [20] E. Komatsu *et al.* [WMAP Collaboration], Astrophys. J. Suppl. **180**, 330 (2009) doi:10.1088/0067-0049/180/2/330 [arXiv:0803.0547 [astro-ph]].
- [21] E. Komatsu *et al.* [WMAP Collaboration], Astrophys. J. Suppl. **192**, 18 (2011) doi:10.1088/0067-0049/192/2/18 [arXiv:1001.4538 [astro-ph.CO]].
- [22] G. Hinshaw *et al.* [WMAP Collaboration], Astrophys. J. Suppl. **208**, 19 (2013) doi:10.1088/0067-0049/208/2/19 [arXiv:1212.5226 [astro-ph.CO]].
- [23] See, <http://www.core-mission.org/>
- [24] P. de Bernardis *et al.* [CORE Collaboration], arXiv:1705.02170 [astro-ph.IM].
- [25] J. Delabrouille *et al.* [CORE Collaboration], arXiv:1706.04516 [astro-ph.IM].
- [26] E. Di Valentino *et al.* [CORE Collaboration], arXiv:1612.00021 [astro-ph.CO].
- [27] F. Finelli *et al.* [CORE Collaboration], arXiv:1612.08270 [astro-ph.CO].
- [28] T. Matsumura *et al.*, J. Low. Temp. Phys. **176**, 733 (2014) doi:10.1007/s10909-013-0996-1 [arXiv:1311.2847 [astro-ph.IM]].
- [29] T. Matsumura *et al.*, J. Low. Temp. Phys. **184**, no. 3-4, 824 (2016). doi:10.1007/s10909-016-1542-8
- [30] A. Kogut *et al.*, JCAP **1107**, 025 (2011) doi:10.1088/1475-7516/2011/07/025 [arXiv:1105.2044 [astro-ph.CO]].
- [31] M. J. Mortonson, C. Dvorkin, H. V. Peiris and W. Hu, Phys. Rev. D **79** (2009) 103519 [arXiv:0903.4920 [astro-ph.CO]].
- [32] W. Hu and G. P. Holder, Phys. Rev. D **68**, 023001 (2003) doi:10.1103/PhysRevD.68.023001 [astro-ph/0303400].

- [33] A. D. Linde, Phys. Rev. D **59**, 023503 (1999) [hep-ph/9807493].
- [34] A. D. Linde, M. Sasaki and T. Tanaka, Phys. Rev. D **59**, 123522 (1999) [astro-ph/9901135].
- [35] M. Joy, V. Sahni, A. A. Starobinsky, Phys. Rev. D **77**, 023514 (2008) [arXiv:0711.1585].
- [36] M. Joy, A. Shafieloo, V. Sahni, A. A. Starobinsky. JCAP **0906**, 028 (2009) [arXiv:0807.3334].
- [37] R. Bousso, D. Harlow and L. Senatore, arXiv:1309.4060 [hep-th]; R. Bousso, D. Harlow and L. Senatore, arXiv:1404.2278 [astro-ph.CO].
- [38] C. R. Contaldi, M. Peloso, L. Kofman and A. D. Linde, JCAP **0307**, 002 (2003) [astro-ph/0303636].
- [39] G. Efstathiou and S. Chongchitnan, Prog. Theor. Phys. Suppl. **163**, 204 (2006) doi:10.1143/PTPS.163.204 [astro-ph/0603118].
- [40] D. K. Hazra, A. Shafieloo, G. F. Smoot and A. A. Starobinsky, Phys. Rev. Lett. **113**, no. 7, 071301 (2014) doi:10.1103/PhysRevLett.113.071301 [arXiv:1404.0360 [astro-ph.CO]].
- [41] D. K. Hazra, L. Sriramkumar and J. Martin, JCAP **1305**, 026 (2013) [arXiv:1201.0926 [astro-ph.CO]].
- [42] See <https://sites.google.com/site/codocosmo/bingo>.
- [43] W. Hu and T. Okamoto, Phys. Rev. D **69**, 043004 (2004) doi:10.1103/PhysRevD.69.043004 [astro-ph/0308049].
- [44] J. Errard, S. M. Feeney, H. V. Peiris and A. H. Jaffe, JCAP **1603**, no. 03, 052 (2016) doi:10.1088/1475-7516/2016/03/052 [arXiv:1509.06770 [astro-ph.CO]].
- [45] P. A. R. Ade *et al.* [BICEP2 and Keck Array Collaborations], Phys. Rev. Lett. **116**, 031302 (2016) doi:10.1103/PhysRevLett.116.031302 [arXiv:1510.09217 [astro-ph.CO]].
- [46] R. Hlozek, J. Dunkley, G. Addison, J. W. Appel, J. R. Bond, C. S. Carvalho, S. Das and M. Devlin *et al.*, Astrophys. J. **749** (2012) 90 [arXiv:1105.4887 [astro-ph.CO]].
- [47] A. Blanchard, M. Douspis, M. Rowan-Robinson and S. Sarkar, Astron. Astrophys. **412**, 35 (2003) [astro-ph/0304237].
- [48] P. Hunt and S. Sarkar, Phys. Rev. D **76**, 123504 (2007) [arXiv:0706.2443 [astro-ph]].
- [49] D. K. Hazra, A. Shafieloo and T. Souradeep, Phys. Rev. D **87**, 123528 (2013) [arXiv:1303.5336 [astro-ph.CO]].
- [50] See, <http://camb.info/>.
- [51] A. Lewis, A. Challinor and A. Lasenby, Astrophys. J. **538** (2000) 473 [astro-ph/9911177].
- [52] See, <http://cosmologist.info/cosmomc/>.
- [53] A. Lewis and S. Bridle, Phys. Rev. D **66** (2002) 103511 [astro-ph/0205436].
- [54] X. H. Fan, C. L. Carilli and B. G. Keating, Ann. Rev. Astron. Astrophys. **44**, 415 (2006) doi:10.1146/annurev.astro.44.051905.092514 [astro-ph/0602375].
- [55] R. J. Bouwens, G. D. Illingworth, P. A. Oesch, J. Caruana, B. Holwerda, R. Smit and S. Wilkins, Astrophys. J. **811**, no. 2, 140 (2015) doi:10.1088/0004-637X/811/2/140 [arXiv:1503.08228 [astro-ph.CO]].
- [56] R. Adam *et al.* [Planck Collaboration], Astron. Astrophys. **596** (2016) A108 doi:10.1051/0004-6361/201628897 [arXiv:1605.03507 [astro-ph.CO]].
- [57] D. K. Hazra and G. F. Smoot, JCAP **1711**, no. 11, 028 (2017) doi:10.1088/1475-7516/2017/11/028 [arXiv:1708.04913 [astro-ph.CO]].
- [58] N. Aghanim *et al.* [Planck Collaboration], Astron. Astrophys. **596** (2016) A107 doi:10.1051/0004-6361/201628890 [arXiv:1605.02985 [astro-ph.CO]].

- [59] M. J. D. Powell, Cambridge NA Report NA2009/06, University of Cambridge, Cambridge (2009).
- [60] M. Ballardini, F. Finelli, C. Fedeli and L. Moscardini, JCAP **1610** (2016) 041 doi:10.1088/1475-7516/2016/10/041 [arXiv:1606.03747 [astro-ph.CO]].